Twentieth Century Tropical Sea Surface Temperature Trends Revisited

Clara Deser and Adam S. Phillips
National Center for Atmospheric Research, Boulder, Colorado

Michael A. Alexander
NOAA/Earth System Research Laboratory, Boulder, Colorado

March 18, 2010 *(Submitted to GRL)*

Abstract

This study compares the global distribution of 20th century SST and marine air temperature trends from a wide variety of data sets including un-interpolated archives as well as globally-complete reconstructions. Apart from the eastern equatorial Pacific, all datasets show consistency in their statistically significant trends, with warming everywhere except the far northwestern Atlantic; the largest warming trends are found in the middle latitudes of both hemispheres. Two of the SST reconstructions exhibit statistically significant cooling trends over the eastern equatorial Pacific, in disagreement with the un-interpolated SST and marine air temperature datasets which show statistically significant warming in this region. Twentieth century trends in tropical marine cloudiness, precipitation and SLP from independent data sets provide physically consistent evidence for a reduction in the strength of the atmospheric Walker Circulation accompanied by an eastward shift of deep convection from the western to the central equatorial Pacific.

1. Introduction

Sea surface temperature (SST), a fundamental physical parameter of the climate system, is well suited for monitoring climate change due to the oceans' large thermal

inertia compared with that of the atmosphere and land. Accurate determination of long-term SST trends is hampered, however, by poor spatial and temporal sampling and inhomogeneous measurement practices (Hurrell and Trenberth, 1999; Rayner et al., 2009). As a result, 20th century SST trends are subject to considerable uncertainty, limiting their physical interpretation and utility as verification for climate model simulations. This uncertainty is especially evident in the tropical Pacific where even the sign of the centennial trend is in question (Vecchi et al., 2008). Given the influence of tropical Pacific SST anomalies on climate worldwide, resolving these discrepancies remains an important task.

Previous studies have focused largely on SST trends from reconstructed data sets. The purpose of this study is to provide a broad assessment of 20th century global SST trends by considering a wide variety of gridded data sources including un-interpolated archives as well as globally complete reconstructions. The SST trends are compared with independently measured night-time marine air temperature (NMAT) trends for evidence of physical consistency. The SST/NMAT trends over the tropical Pacific are further evaluated in the context of trends in tropical cloudiness, precipitation, and sea level pressure.

2. Data and Methods

Global SST trends since 1900 are computed for 5 different datasets: Hadley Centre SST version 2 (HadSST2; Rayner et al., 2006); Minobe and Maeda (2005); Hadley Centre sea ice and SST version 1 (HadISST1; Rayner et al., 2003); National Oceanic and Atmospheric Administration Extended Reconstructed SST version 3

(ERSSTv3b; Smith et al., 2008); and Kaplan Extended SST version 2 (Kaplanv2; Kaplan et al., 1998). HadSST2 and Minobe/Maeda (both on a 2ºx2º latitude/longitude grid) are based on the International Comprehensive Atmosphere-Ocean Data Set (ICOADS) and employ different quality-control and bias correction procedures; no "analysis" of the data is performed (e.g., no spatial or temporal smoothing or interpolation) and missing grid boxes are not filled in. HadISST1 (1ºx1º), ERSSTv3b (2ºx2º), and Kaplanv2 (5ºx5º) are analysis products which use different optimal statistical procedures to smooth the data and fill in missing values; further information is given in the cited references.

In addition to SST, we compute trends in night-time marine air temperatures (NMAT) from Meteorological Office Historical Marine Air Temperature version 4 (MOHMAT4; Rayner et al., 2003) and terrestrial air temperatures from Hadley Centre/Climate Research Unit Temperature version 3 variance-adjusted (HadCRUT3v; Brohan et al., 2005). Both datasets are on a 5º x 5º grid, and like HadSST2 missing grid boxes are not filled in and no "analysis" of the data is performed. It should be noted that MOHMAT4, HadCRUTv3 and HadSST2 are independent in that they consist of measurements from different observational platforms or instruments (N. Rayner, personal communication, 2010). Over the tropics, we also compute trends in land station precipitation from Hulme et al. (1998), total cloud amount and sea level pressure (SLP) from ICOADS version 2.4 (Woodruff et al., 2008), and SLP from Hadley Centre SLP version 2 (Allan and Ansell, 2006). The Hulme (2.5º x 3.75º) and ICOADS (2º x 2º) data are neither smoothed nor interpolated, while HadSLP2 (5º x 5º) is a globally complete optimal reconstruction based on terrestrial station records and marine observations from ICOADS.

We calculate linear trends from monthly anomalies using the method of least-squares, and assess their statistical significance using a Student's-t test and taking into account serial autocorrelation based on the method of Zwiers and von Storch (1995).

3. Results

a. Data Coverage

In order to discriminate between secular climate change and naturally-occurring multi-decadal variability, it is important to consider as long a period of record as possible. Seeking a balance between adequate data coverage (see Fig. 1 in the Supplemental Materials) and length of record, we have examined SST trends using a variety of start dates (1900, 1910 and 1920) and data sampling thresholds; all of the results discussed below are robust to the different choices. In the figures that follow, we show trend maps based on the period 1900-2008 using a 3 month per decade threshold; trends based on 1920-2008 using a 24 month per decade threshold are shown in Fig. 2 of the Supplemental Materials. We emphasize that although our sampling criterion is lenient, we rely on additional factors such as regional coherency (note that no additional spatial smoothing has been applied to any of the data sets) and consistency with independently measured marine air temperatures to assess the reality of the SST trends.

b. Global SST trends

The 20th century SST trend distributions from the 5 different data sets are compared in Fig. 1 for the period 1900 to 2008 (2002 for Minobe/Maeda, the latest year available), along with air temperature trends based on HadCRUTv3 over land and

MOHMAT4 over the oceans for the period 1900 to 2005 (the latest year available). The SST trends from the un-interpolated HadSST2 and Minobe/Maeda archives are similar, exhibiting positive values everywhere except the western portion of the northern North Atlantic. The largest warming trends (approximately 1.2-1.6 ºC per century) occur directly east of the continents in the northern hemisphere, in the Southern Ocean and the eastern tropical Atlantic. The eastern tropical Pacific warms by approximately 0.8-1.0 ºC per century, similar in magnitude to the tropical Indian Ocean and the central tropical Atlantic. Trends in NMAT from the un-interpolated MOHMAT4 dataset corroborate those in SST from HadSST2 and Minobe/Maeda, with generally similar large-scale patterns and amplitudes. The agreement between NMAT and SST, physically related quantities from independent data sets, provides strong support for the reality of their trends. Another important confirmation of the marine NMAT trends is their coherence with independent air temperature trends over nearby land areas from HadCRUT3v. For example, the terrestrial warming over the islands of Indonesia and coastal regions of Australia, South America, South Africa, North America, Europe, and eastern Asia is remarkably similar in amplitude to the air temperature increases over the adjacent oceanic regions (even the cooling at the southern tip of Greenland agrees with the cooling over the far north Atlantic). There are a few isolated areas where the air temperature trends over land do not match those over nearby maritime areas, for example Madagascar, the southeastern United States, and northern Chile.

The 3 reconstructed SST data sets (ERSSTv3b, HadISST1, and Kaplanv2) exhibit broad similarity in their trend patterns and amplitudes, as well as overall agreement with the un-interpolated SST data sets, with the notable exception of the central and eastern

equatorial Pacific. In this region, HadISST1 and Kaplanv2 exhibit weak but significant cooling while ERSSTv3b shows significant warming, the latter in agreement with HadSST2, Minobe/Maeda, and MOHMAT4. The discrepancy between HadISST1 and ERSST was highlighted by Vecchi et al. (2008; see also Hurrell and Trenberth, 1999).

c. Tropical climate trends

Trends in tropical marine cloudiness from ICOADS, land station precipitation from Hulme, and SLP from ICOADS and HadSLP2r are shown in Fig. 2; SST trends from HadISST1 and HadSST2 are also shown for reference. All trends are computed based on monthly anomalies beginning in 1900 and ending in 2008 (2006 for ICOADS) except for precipitation which uses a start date of 1920 due to insufficient data coverage before that time and an end date of 1996, the last year of data available. As in Fig. 1, no spatial smoothing has been applied to any of the trend maps. Changes in observing practice may have caused spurious increases in ICOADS cloudiness (Norris, 1999). Following Deser and Phillips (2006), we account for these artificial trends by removing the tropical (30ºN - 30ºS) mean cloudiness trend from each oceanic grid box. The resemblance of the spatial patterns of land station precipitation and residual cloudiness trends provides strong evidence for the spurious nature of the tropical mean cloudiness trend (Fig. 2).

The distribution of residual cloudiness trends exhibits positive values (0.8 – 1.4 oktas per century) over the central equatorial Pacific accompanied by negative values over the western equatorial Pacific (-0.4 – -0.8 oktas per century). This pattern is reminiscent of the cloudiness (and precipitation) changes that occur in association with El

144 Nino events (Deser et al., 2004) and the 1976/77 climate regime "shift" (Deser and
145 Phillips, 2006). Negative cloudiness trends are also found over the western Indian
146 Ocean, the Pacific Inter-Tropical Convergence Zone (ITCZ) east of 135ºW and the
147 subtropical eastern Pacific and Atlantic. Precipitation trends are generally consistent with
148 residual cloudiness trends in regions where the two data sets overlap: in particular,
149 positive precipitation trends are found at island stations in the central equatorial Pacific
150 between 160ºE and 140ºW, and negative trends to the west between130ºE and 160ºE.
151 SLP trends from ICOADS are generally positive over the tropical Indian Ocean and
152 western Pacific, and a mixture of negative and positive values over the eastern Tropical
153 Pacific. The smoother HadSLP2r trends corroborate the large-scale pattern evident in
154 ICOADS, and are indicative of a weakening of the SLP gradient between the eastern
155 Pacific and the Indian Ocean/West Pacific. Collectively, the independent trends in marine
156 cloudiness, precipitation and SLP provide physically consistent evidence for a reduction
157 in the strength of the atmospheric Walker Circulation accompanied by an eastward shift
158 in convection from the western to the central equatorial Pacific.

159 Based on the maps shown in Fig. 2, we formed the following regional time series:
160 eastern equatorial Pacific SST (1ºN - 1ºS, 170ºW - 90ºW) from HadSST2[1]; central
161 equatorial Pacific cloudiness (6ºN - 12ºS, 165ºE - 150ºW) minus central north Pacific
162 cloudiness (18ºN - 6ºN, 165ºE - 150ºW) from ICOADS; and Indian Ocean/West Pacific
163 SLP (20ºN - 20ºS, 30ºE - 150ºE) minus eastern Pacific SLP (20ºN - 20ºS, 180º - 70ºW)
164 from ICOADS. These indices are not sensitive to the precise definitions of the regions
165 except for cloudiness, which exhibits some differences in the first few decades of the 20th

[1] A narrow equatorial box is used for later comparison with HadISST1, but similar results are obtained for 5ºN - 5ºS.

166 century (not shown); similar regions were used for characterizing Pacific multi-decadal
167 variability in Deser et al. (2004). These indices are displayed in Fig. 3 using various
168 degrees of temporal smoothing to emphasize different aspects of the variability.

169 Although the raw monthly anomaly time series exhibit considerable high
170 frequency noise, they are coherent on interannual and longer time scales and exhibit
171 prominent ENSO variability throughout the record. The main periods of disagreement
172 occur in association with high levels of noise due to paucity of data especially during the
173 first two decades and World War II. The correlation coefficients between each pair of
174 indices (marked directly on Fig. 3) are all significant at the 99% level: the 0.66
175 correlation between the SST and SLP records is particularly noteworthy given the large
176 number of data points and lack of temporal smoothing. There is also strong
177 correspondence among the 12-month running mean records, with 95% significant
178 correlations of 0.61-0.91. The 20-year low-pass filtered records also exhibit high
179 correlations (0.86-0.95) reflecting consistency in their multi-decadal fluctuations as well
180 as in their overall upward trends. Note that the trends constitute only a small fraction of
181 the total variability of the raw monthly anomaly time series and less than half of the
182 variability on time scales longer than 20 years. Strong correspondence between two
183 canonical SLP and SST records of ENSO dating back to 1877 was shown by Bunge and
184 Clarke (2009) using more sophisticated analysis techniques.

185 The disagreement in sign between the trends in HadSST2 and HadISST1 in the
186 eastern equatorial Pacific is readily apparent by comparing their 20-year low-pass filtered
187 records (Fig. 3). Note that the two SST indices agree well on inter-annual and multi-
188 decadal timescales (correlation coefficients of 0.95 for detrended 12-month running

means and 0.90 for detrended 20yr lowpass filtered data): only their long term trends differ. The correlations between the 20-yr lowpass filtered equatorial Pacific SST index based on HadISST1 and the cloudiness and SLP records shown in Fig. 3 (0.38 and 0.50, respectively) are substantially lower than those based on HadSST2 (0.86 and 0.95, respectively).

4. Summary and Discussion

We have evaluated 20th century (1900 to approximately 2008) SST trends from a variety of data sources including un-interpolated archives as well as globally complete reconstructions. Statistically significant SST trends from the two un-interpolated datasets (HadSST2 and Minobe/Maeda) are positive everywhere except the northern North Atlantic, with magnitudes approximately 0.4-1.0 ºC per century in the tropics and subtropics and 1.2-1.6 ºC per century at higher latitudes. These SST trends are corroborated by independently measured NMAT trends from the un-interpolated MOHMAT4 dataset and by terrestrial air temperature trends at coastal locations from the un-interpolated HadCRUT3v archive. SST trends from the reconstructed datasets (ERSSTv3b, HadISST1 and Kaplanv2) are generally similar to those from the un-interpolated archives with the notable exception of the tropical Pacific which exhibits cooling in HadISST1 and Kaplanv2.

The intensified warming trends off the east coasts of China and northern North America and over the northern North Pacific may be related to the relatively shallow bathymetry and associated ocean mixed layer depths as suggested by Xie et al. (2002). In addition, advection of continental air temperature trends by the prevailing westerlies and

212 a reduction in cloud cover (not shown) may play a role. The cooling trend directly south
213 of Greenland may be related to the century-long upward trend in the North Atlantic
214 Oscillation via the associated increase in wind speed and resulting heat loss from the
215 ocean surface. Enhanced warming over the Southern Ocean may be due in part to a
216 decrease in cloud cover (not shown). Alternatively, the pattern of cooling in the far north
217 Atlantic coupled with warming in the Southern Ocean may be a signature of a weakened
218 oceanic thermohaline circulation in response to global warming. Further work is needed
219 to assess the mechanisms responsible for the spatial distribution of the 20th century SST
220 trends.

221 The HadISST1 and Kaplanv2 reconstructions disagree with ERSSTv3b and the
222 un-interpolated datasets on the sign of the SST trend in the eastern equatorial Pacific.
223 Independent NMAT measurements show a warming trend in this region that is very close
224 in magnitude to that from HadSST2 (0.36 ºC compared to 0.35 ºC per century). Given
225 that marine air temperature and SST anomalies are physically constrained by surface
226 energy exchange, the agreement between NMAT and HadSST2 provides strong support
227 for the reality of the warming trend in the eastern equatorial Pacific. Though the trends in
228 HadISST1 and Kaplanv2 over the eastern equatorial Pacific appear to be erroneous, their
229 interannual to decadal variations are in agreement with those in HadSST2 and NMAT
230 (correlation coefficients of 0.95 and 0.92, respectively, based on detrended 12-month
231 running mean anomalies for the region 1ºN - 1ºS, 170ºW - 90ºW). Our results have
232 implications for the design of atmospheric model experiments forced with observed SST
233 trends. In particular, specifying the 20th century trend component from HadISST1 or

234 Kaplanv2 in the eastern tropical Pacific may lead to an unrealistic atmospheric circulation
235 response.

236 Centennial trends in tropical marine cloudiness, precipitation, and SLP from
237 independent data sources were also evaluated. These additional climate parameters were
238 shown to exhibit physically consistent trends consisting of a weakening of the zonal SLP
239 gradient between the eastern Pacific and the Indian Ocean/western Pacific accompanied
240 by an eastward shift of cloudiness and precipitation from the western to the central
241 equatorial Pacific. The causal relationship between the tropical Pacific SST and
242 atmospheric circulation trends is open to interpretation. On the one hand, a weakening of
243 the atmospheric Walker Circulation is expected to occur in response to increasing GHG
244 concentrations, even with a zonally uniform warming of the tropical oceans, as discussed
245 by Vecchi and Soden (2007). In this view, the role of tropical ocean dynamics is to
246 reduce the amplitude of both the Walker Circulation change and the warming in the
247 eastern equatorial Pacific. Alternatively, the physical paradigm for ENSO holds that a
248 weakening of the zonal SLP gradient (e.g., the Walker Circulation) is accompanied by a
249 weakening of the zonal SST gradient (more warming in the eastern compared to the
250 western equatorial Pacific) due to the Bjerknes feedback mechanism. Both mechanisms
251 could contribute to the observed centennial trends documented in this study.

252 Recently, Karnauskas et al. (2009) reported that the HadISST1, Kaplanv2 and
253 ERSSTv3b reconstructions all exhibit a strengthening of the east-to-west SST gradient
254 across the equatorial Pacific during the 20th century, despite disagreeing on the sign of the
255 SST trend in east. However, only the month of September showed a statistically
256 significant strengthening for ERSSTv3b, compared to June-January (July-January) for

HadISST1 (Kaplanv2). Using data from all months of the year, we find no evidence for a statistically significant strengthening of the zonal gradient in ERSSTv3b, HadSST2, Minobe/Maeda, or MOHMAT4. Further, we emphasize that data coverage constraints make it difficult to accurately determine the 20th century trend in the zonal SST gradient across the equatorial Pacific (Fig. 1 of the Supplemental Materials), and indeed no such determination is possible when a 20% threshold (24 months per decade) is used for computing the trends since 1920 (Fig. 2 of the Supplemental Materials).

Characterizing the pattern and amplitude of SST trends over the past century remains a challenge due to observational uncertainties associated with limited data sampling, changing measurement techniques and analysis procedures. Thus, there is a continuing need for refining and improving the development of homogeneous gridded SST data sets and associated globally-complete reconstructions for climate change research following the recommendations in Rayner et al. (2009).

Acknowledgments

We thank Drs. Lucia Bunge, Allan Clarke, Matt Newman, Yuko Okumura, Nick Rayner and Kevin Trenberth for useful discussions during the course of this work. We also appreciate the comments of two anonymous reviewers on a previous draft.

References

Allan, R. J. and Ansell, T. J., 2006: A new globally complete monthly historical mean sea level pressure data set (HadSLP2): 1850-2004. *J. Clim.,* 19, 5816-5842.

280 Brohan et al., 2005: Uncertainty estimates in regional and global observed temperature
281 changes: a new dataset from 1850. *J. Geophys. Res*, 111, D12106,
282 doi:10.1029/2005JD006548.
283
284 Bunge, L. and A.J. Clarke, 2009: A verified estimate of the El Nino Index Nino-3.4 since
285 1877. *J. Clim*., 22, 3979-3992.
286
287 Deser, C., A.S. Phillips and J.W. Hurrell, 2004: Pacific interdecadal climate variability:
288 linkages between the Tropics and the North Pacific during boreal winter since 1900. *J.*
289 *Clim.*, 17, 3109–3124.
290
291 Deser, C., and A. S. Phillips, 2006: Simulation of the 1976/1977 climate transition over
292 the North Pacific: Sensitivity to tropical forcing. *J. Climate*, 19, 6170-6180.
293
294 Hulme M., T. J. Osborn, and T. C. Johns, 1998: Precipitation sensitivity to global
295 warming: Comparison of observations with HadCM2 simulations. *Geophys. Res. Lett*, **25**,
296 3379–3382.
297
298 Kaplan et al., 1998: Analyses of global sea surface temperature 1856-1991. *J. Geophys.*
299 *Res*., 103, 18,567-18,589.
300
301 Norris J. R., 1999: On trends and possible artifacts in global ocean cloud cover between
302 1952 and 1995. *J. Climate*, **12**, 1864–1870.

Rayner et al., 2003: Global analyses of sea surface temperature, sea ice, and night marine air temperature since the late nineteenth century. *J. Geophys. Res*., 108, No. D14, 4407, doi:10.1029/2002JD002670, 2003

Rayner et al., 2006: Improved analyses of changes and uncertainties in sea surface temperature measured in situ since the mid-nineteenth century: the HadSST2 data set. *J. Clim.*, 19, 446-469.

Rayner et al., 2009: Evaluating Climate Variability and Change From Modern and Historical SST Observations" in *Proceedings of OceanObs'09: Sustained Ocean Observations and Information for Society (Vol. 2),* Venice, Italy, 21-25 September 2009, Hall, J., Harrison D.E. & Stammer, D., Eds., ESA Publication WPP-306.

Smith et al., 2008: Improvements to NOAA's historical merged land-ocean surface temperature analysis (1880-2006). *J. Clim.*, 21, 2283-2296.

Vecchi, G. A., A. Clement, and B. J. Soden, 2008: Pacific signature of global warming: El Niño or La Niña?, *Eos Trans. AGU*, 89(9), 81-83.

Vecchi, G.A., and B.J. Soden, 2007: Global Warming and the Weakening of the Tropical Circulation. *J. Clim.*, 20, 4316–4340.

326 Woodruff et al., 2008: The evolving SST record from ICOADS. In Climate Variability
327 and Extremes during the Past 100 Years (Broennimann et al., Eds.), in *Global Change*
328 *Research*, 33, Springer, 65-83.
329
330 Zwiers, F.W., and H. von Storch, 1995: Taking serial correlation into account in tests of
331 the mean. *J. Clim.*, 8, 336–351.
332

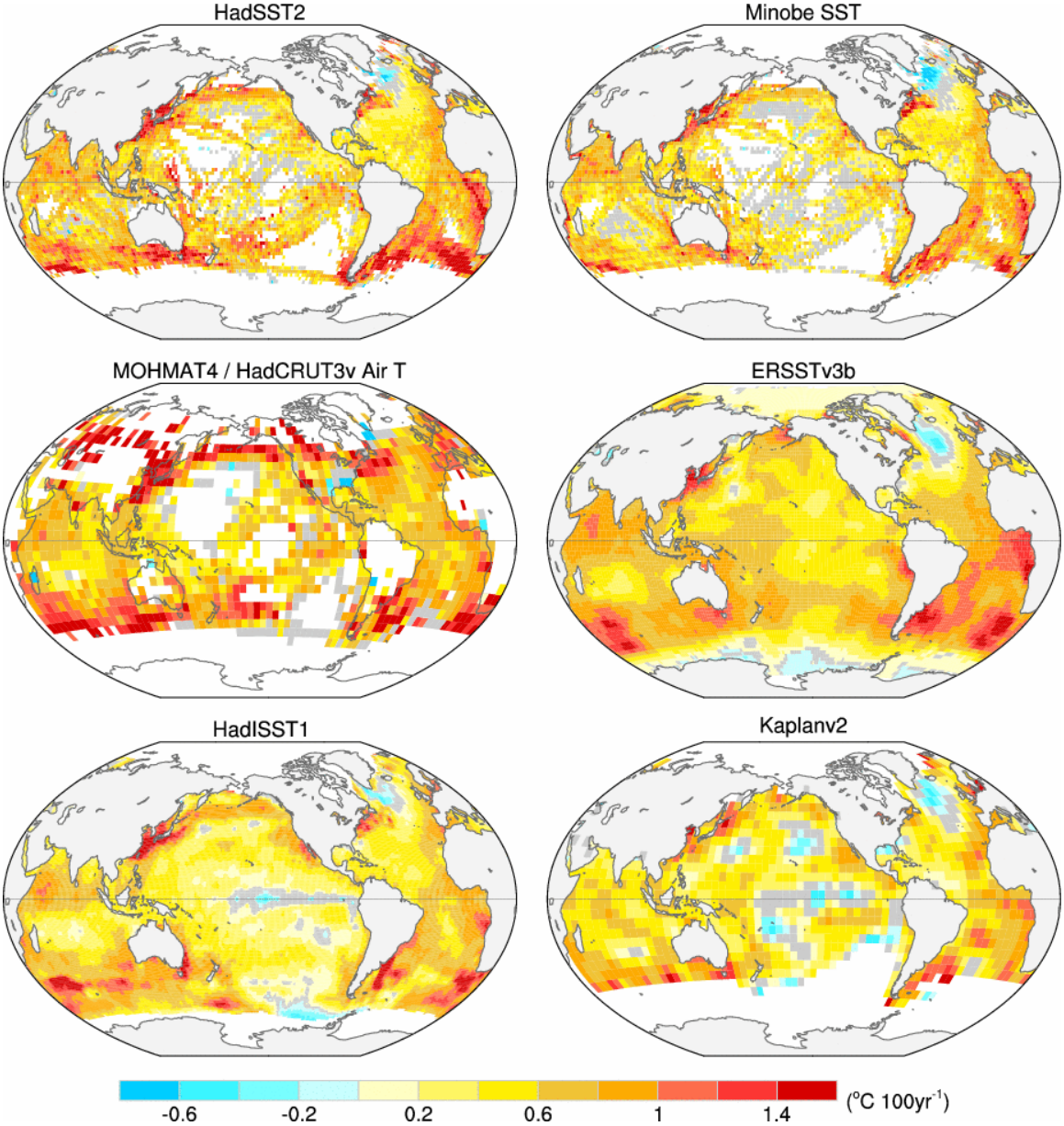

332

333 **Figure 1.** Twentieth century SST trends (ºC per century) computed from monthly
334 anomalies since 1900 for various data sets as indicated. White grid boxes denote
335 insufficient data, and gray boxes indicate trends that are not statistically significant at the
336 95% confidence level. See text for additional information.

337

338

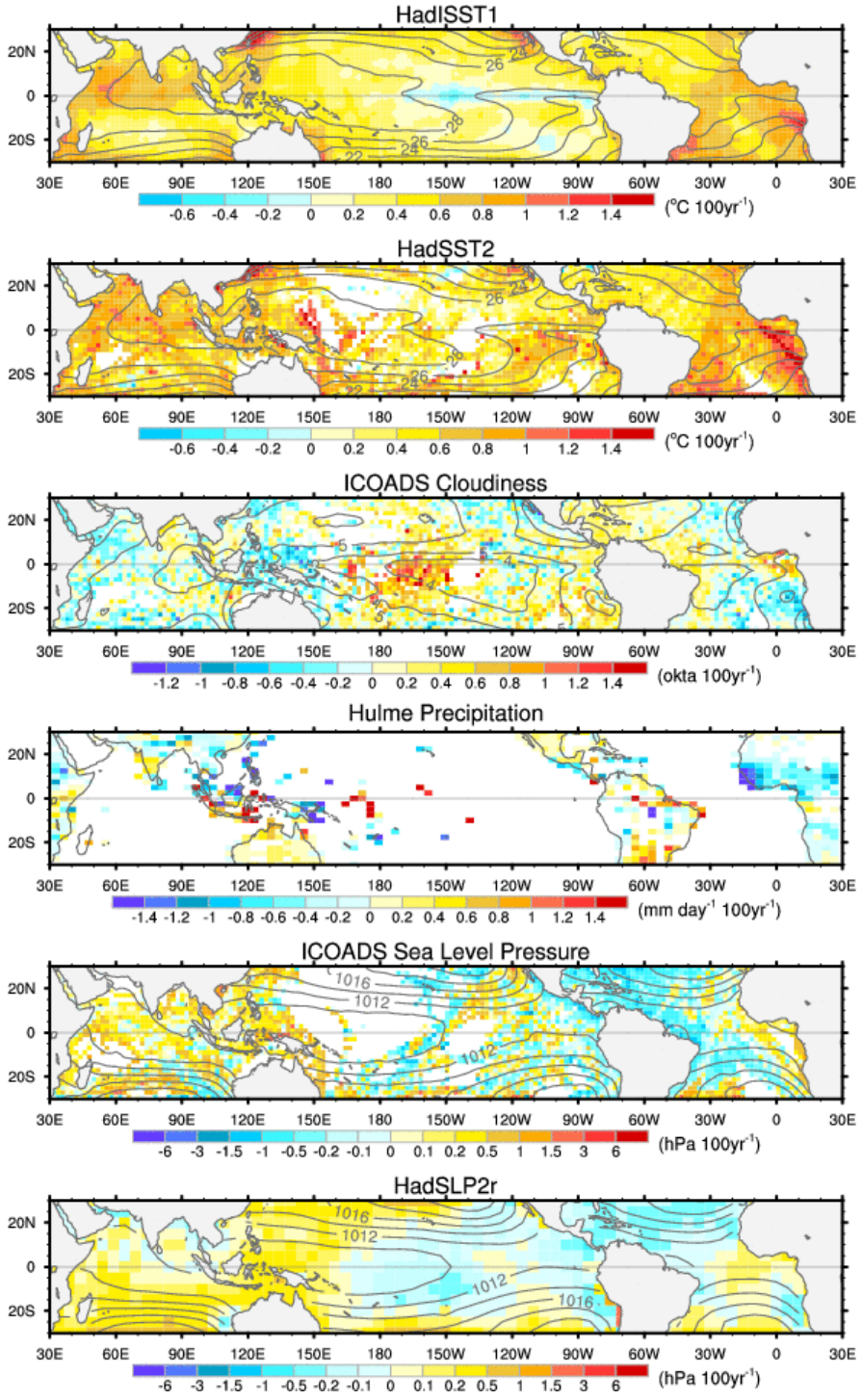

Figure 2. Twentieth century tropical climate trends from a variety of data sources as indicated. White grid boxes denote insufficient data. See text for additional information.

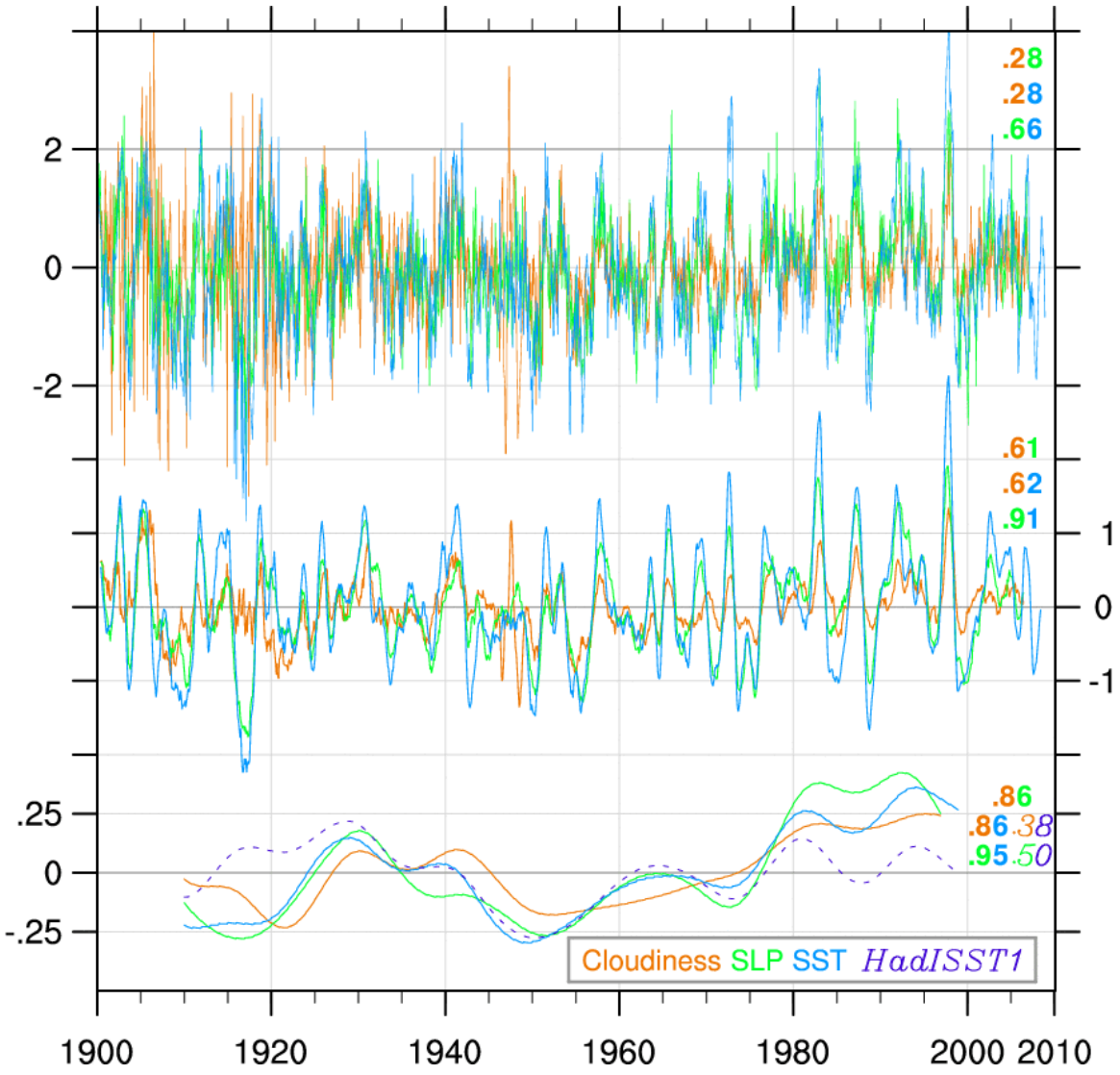

Figure 3. Monthly anomaly time series for selected regional tropical climate indices (see text for definitions). Blue and purple denote SST (ºC) from HadSST2 and HadISST1, respectively; orange denotes cloudiness (oktas); and green denotes SLP (hPa). The top, middle and bottom sets of curves show the raw, 12-month running mean, and 20-year low-pass filtered monthly anomaly time series, respectively. Color coded numbers to the right of each set of curves denote correlation coefficients between each pair of indices (e.g., an orange and blue numeral gives the correlation between cloudiness and SST).

365 ***Auxiliary Material for***
366
367 **Twentieth Century Tropical Sea Surface Temperature Trends Revisited**
368
369 Clara Deser and Adam S. Phillips
370 *National Center for Atmospheric Research, Boulder, Colorado*
371
372 Michael A. Alexander
373 *NOAA/Earth System Research Laboratory, Boulder, Colorado*
374
375 March 18, 2010 *(submitted to GRL)*
376
377

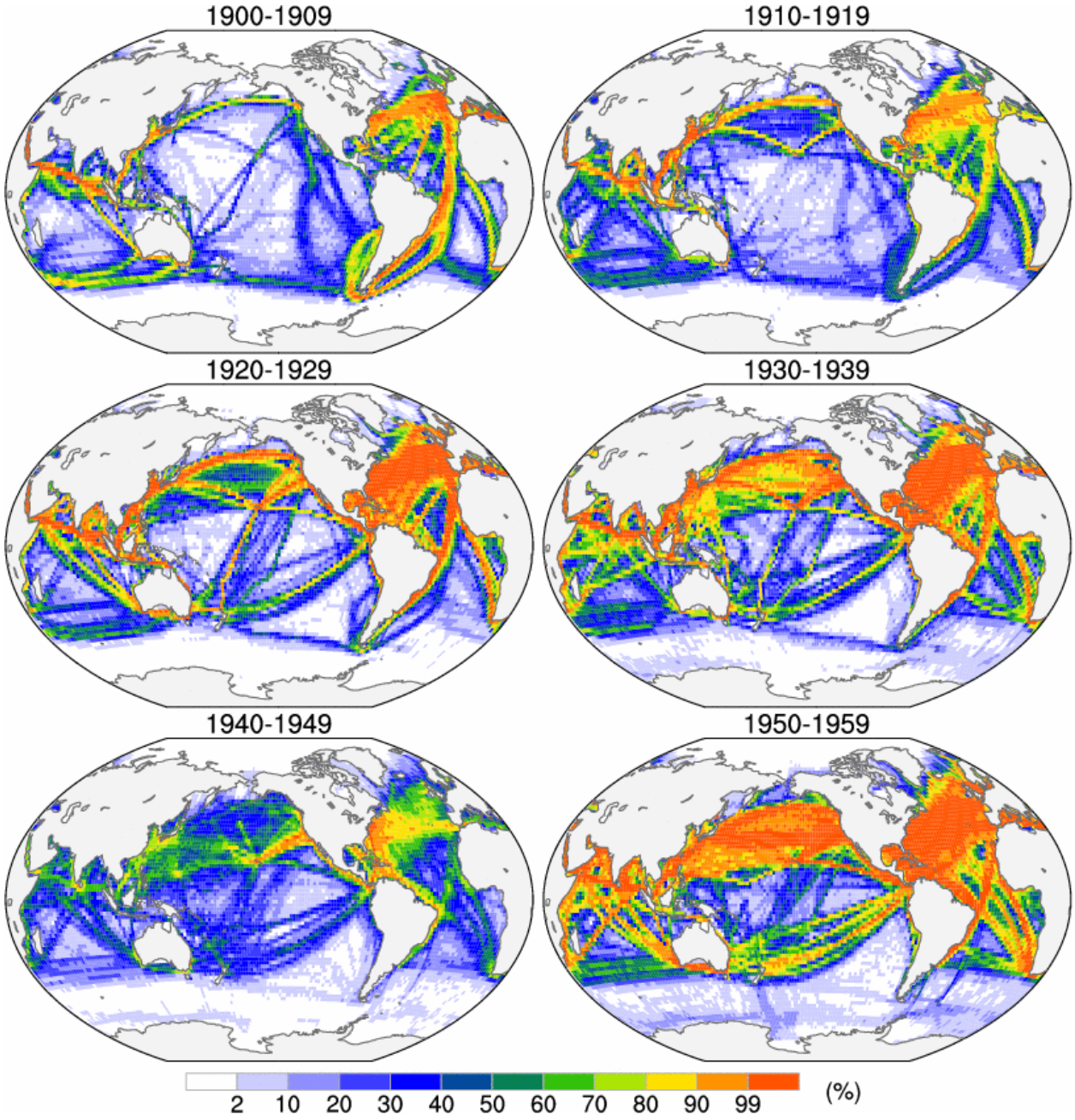

Figure 1. Distribution of SST observations from HadSST2, shown as the percent of months with at least 1 observation per 2º latitude x 2º longitude grid box during each decade as indicated.

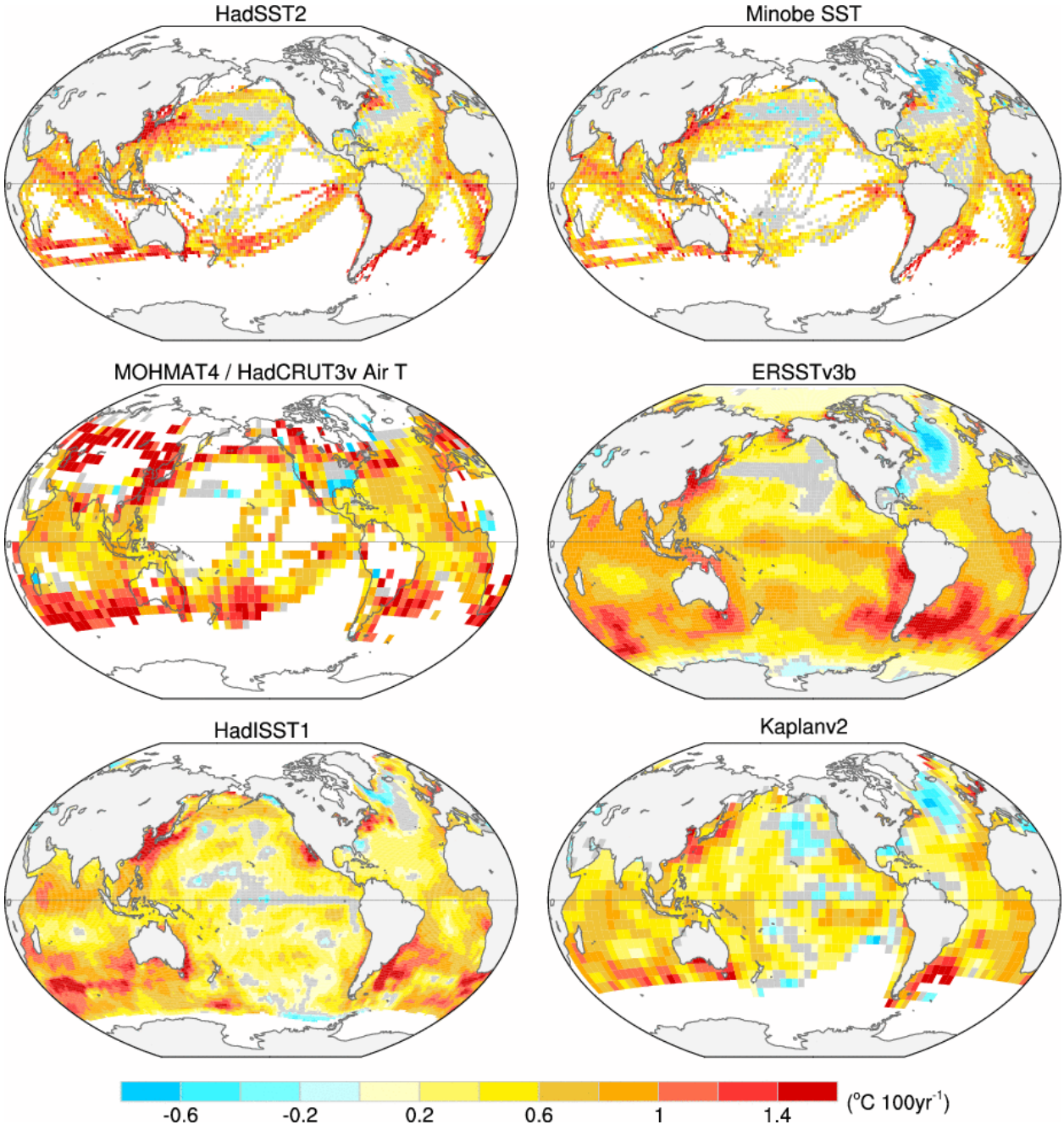

Figure 2. Twentieth century SST trends (ºC per century) computed from monthly anomalies since 1920 for various data sets as indicated. White grid boxes denote insufficient data, and gray boxes indicate trends that are not statistically significant at the 95% confidence level. A minimum of 24 months per decade was required to compute the trends.